Published in final edited form as:
IEEE Trans Biomed Eng. 2012 January ; 59(1): 45–49. doi:10.1109/TBME.2011.2161988.

In-vivo imaging and spectroscopy of dynamic metabolism using simultaneous ^{13}C and ^{1}H MRI

Matthew R Smith,
Department of Medical Physics, University of Wisconsin, Madison, WI 53705 USA

Eric T Peterson,
Department of Medical Physics, University of Wisconsin, Madison, WI 53705 USA

Jeremy W. Gordon,
Department of Medical Physics, University of Wisconsin, Madison, WI 53705 USA

David J. Niles,
Department of Medical Physics, University of Wisconsin, Madison, WI 53705 USA

Ian J. Rowland,
Department of Medical Physics, University of Wisconsin, Madison, WI 53705 USA

Krishna N. Kurpad, and
Department of Medical Physics, University of Wisconsin, Madison, WI 53705 USA

Sean B. Fain
Department of Medical Physics, University of Wisconsin, Madison, WI 53705 USA (phone: 608-263-0090; fax: 608-265-9840

Matthew R Smith: mrsmith4@wisc.edu; Eric T Peterson: etpeterson@wisc.edu; Jeremy W. Gordon: jwgordon@wisc.edu; David J. Niles: djniles@wisc.edu; Ian J. Rowland: irowland@wisc.edu; Krishna N. Kurpad: kurpad@wisc.edu; Sean B. Fain: sbfain@wisc.edu

Abstract

Hyperpolarized (HP) ^{13}C-labeled pyruvate studies with Magnetic Resonance (MR) have been used to observe the kinetics of metabolism *in-vivo*. Kinetic modeling to measure metabolic rates *in-vivo* is currently limited because of nonspecific hyperpolarized signals mixing between vascular, extravascular, and intracellular compartments. In this work simultaneous acquisition of both ^{1}H and ^{13}C signals after contrast agent injection is used to resolve specific compartments to improve the accuracy of the modeling. We demonstrate a novel technique to provide contrast to the intracellular compartments by sequential injection of HP [1-^{13}C] pyruvate followed by gadolinium-chelate to provide T_1-shortening to extra-cellular compartments. A kinetic model that distinguishes the intracellular space and includes the T_1-shortening effect of the gadolinium-chelate can then be used to directly measure the intracellular ^{13}C kinetics.

Index Terms

intracellular; magnetic resonance; metabolism; pyruvate; gadolinium

I. Introduction

Advances in speed and sensitivity of medical imaging modalities such as Magnetic Resonance (MR) Imaging have made it possible to perform a wide range of functional measures *in-vivo* using modeling. One promising technique that has emerged uses hyperpolarized (HP) ^{13}C-labeled pyruvate and other metabolites with MR to observe metabolism in order to determine the relative rates of metabolite production in healthy and

diseased tissues, most notably cancer. No other imaging technology is capable of similar sensitivity for measuring dynamic *in-vivo* metabolism.

In the majority of studies, qualitative ratios, such as lactate to pyruvate peak ratio [1–3], have been used instead of precise quantitative measures of intracellular lactate production from intracellular pyruvate substrate. More recently, simplified models have yielded estimates of metabolic rate constants that indicate a response to treatment [4, 5]. These rates, however, reflect not only intracellular chemical exchange but also membrane transport and pyruvate delivery outside the cell and within the vasculature because of the lack of any contrast between these compartments.

In cell culture, Harris et al. [6] removed the extracellular space through flushing the bioreactor with a perfusion system leaving cells and their intracellular compartments unchanged. Results indicated that label flux estimated with kinetic modeling in T47D cells is chiefly determined by cellular uptake via monocarboxylate transporters (MCTs). Techniques to provide contrast between functional compartments *in-vivo* include frequency shift agents [7], or suppression of flowing spins in the vasculature using stimulated echoes [8]. However, these methods are limited because of high cytotoxicity or because of limited effect at the scale of the organ tissues where cellular measures of metabolism occur.

To separate membrane transport dynamics and intracellular chemical exchange, we present a technique to eliminate the ^{13}C signal within specific compartments by following the injection of HP [1-^{13}C] pyruvate with an injection of a T_1-shortening contrast agent (CA). Using a widely used two-compartment model [4], we show this sequential injection technique avoids an underestimation of the metabolic rate constants by eliminating the relatively large ^{13}C vascular signal in application to healthy rat brain metabolism. Moreover, simultaneous ^{1}H and ^{13}C MRI enables coincident measurement of the CA concentration from the ^{1}H signal to constrain the modeling of the [1-^{13}C] pyruvate metabolism.

II. Methods and materials

A. Hyperpolarized [1-^{13}C] Pyruvate

The process of dynamic nuclear polarization (DNP) has been reported previously [9], [10]. Briefly, 30uL of 14.2M [1-^{13}C] pyruvic acid is doped with 15mM trityl radical (OX63) [9] and inserted into a HyperSense polarizer (Oxford Instruments, Tubney Woods, Abingdon, UK) which provides the 3.35T magnetic field and a temperature of 1.4K. After reaching a solid-state polarization near 20%, rapid dissolution of the [1-^{13}C] pyruvic acid is accomplished by heating a 4 mL solvent (100 mM NaOH, 100 mM Tris, and 0.43 mM EDTA) to 180°C under high pressure. This mixture serves to both thaw and neutralize the pyruvate, making it suitable for animal injection.

B. Gadolinium as an Intracellular Contrast Agent

Gadolinium-chelated compounds are routinely injected clinically to provide tissue contrast by increasing the relaxation rate of surrounding spins during a T_1-weighted acquisition [12]. Although increasing the relaxation rate of a hyperpolarized compound appears at first glance to be an inefficient use of the polarized signal because of the induced accelerated T_1 decay, the restricted distribution of the CA to be intravascular-only in healthy brain and intra and extra-vascular only in most other tissues enables more precise localization of polarized signal and allows a more accurate estimation of intracellular lactate production. Exposure to sufficient concentrations of gadolinium can therefore effectively eliminate all but the compartmental signal [13] without the CA in analogy to the washout experiments performed in cell-culture by Harris *et al.* in Ref [6]. As such, we rely on the restricted distribution of the CA to improve the modeling accuracy of *in-vivo* intracellular metabolism.

C. Animal Preparation

In-vivo studies were performed on adult Sprague-Dawley rats (~230 g) under protocols approved by the Institutional Animal Care and Use Committee using spectroscopy (two rats) and imaging (one rat). Anesthesia was induced with 5% isoflurane and maintained with 2 – 2.5% isoflurane during the experiments. The tail vein was cannulated for intravenous injections. Animals were placed on a heated water pad (Adroit Medical Systems, Loudon, TN) to maintain a body temperature of at least 34°C throughout the experiment. Respiratory rate and rectal temperature were monitored throughout the experiments with an MR-compatible monitoring system (SA Instruments, Inc., Stony Brook, NY).

D. Magnetic Resonance Hardware and Methods

In a series of feasibility studies, two rats were each tested using a spectroscopy acquisition after both a [1-^{13}C] pyruvate injection and after [1-^{13}C] pyruvate injection with sequential CA injection. A third rat was tested using dynamic spectroscopic imaging of both ^{13}C and ^{1}H nuclei after [1-^{13}C] pyruvate and sequential CA injection, i.e. simultaneous multi-nuclear acquisition. For all experiments a 1.2 mL sample of 100 mM hyperpolarized [1-^{13}C] pyruvate was injected at a rate of 0.25 mL/s and was immediately flushed with saline to clear the injection line. In experiments using a sequential injection of CA (Omniscan, GE Healthcare, Milwaukee, WI) a dose of 0.5 mmol/kg was injected through the tail vein 20 seconds after the start of the pyruvate injection to coincide with the maximum signal intensity of lactate followed by a saline flush.

All measurements were performed on a 4.7T small animal scanner with a 10 cm diameter bore (Agilent, Santa Clara, California, USA). For the two dynamic MR spectroscopy experiments, a small 2.2 cm diameter loop surface coil operating at 199.75 MHz for proton was placed directly on the head and used to localize and shim on the brain. This coil was then replaced with a second loop surface coil with identical dimensions operating at 50.23 MHz for the carbon acquisition. The sensitivity of the loop coil restricted the acquired signal to the brain due to its limited diameter. Dynamic spectroscopy began ~2s prior to the injection of the hyperpolarized [1-^{13}C] pyruvate. A flip angle (approximately 8°) was used to produce a free induction decay every 2 seconds (TR = 2 s) consisting of 800 readout points and a spectral window of 4000 Hz. A small urea reference phantom (5 mL of 3 M, 99% ^{13}C enriched urea) was placed above the coil.

The dynamic MR spectroscopic imaging (MRSI) experiment used a simultaneous ^{13}C and ^{1}H acquisition with a custom built dual-tuned orthogonal double solenoid (ODS) RF volume coil which was designed specifically for this application [14]. The organ of interest was the liver for this experiment, and all other aspects of the setup were the same as previously described.

E. Data Acquisition and Analysis

The resulting spectra were apodized in the time domain using a Blackman-Harris window [15]. Zero- and first-order phasing was applied by minimizing the entropy [16] using custom scripts in Matlab (The Mathworks, Natick, MA). After normalizing the data to the maximum pyruvate signal, the peak signals were plotted over time.

The simultaneous ^{13}C and ^{1}H imaging acquisition consists of a fast 2D radial imaging acquisition with the receiver channels and modification of the signal mixer of the scanner to demodulate separately at both the ^{13}C and ^{1}H nuclear magnetic resonance frequencies [17]. This allows for an imaging sequence which acquires the same imaging volume in time and space enabling reconstruction of both a dynamic CA concentration [CA] map as well as the dynamic ^{13}C metabolic map.

F. Compartmental Modeling

The dynamic signals for the pyruvate and lactate peaks were fitted to a well described two-compartment model [4] that is consistent with intracellular pyruvate to lactate conversion:

$$dL_Z/dt = -\rho_L(L_Z - L_\infty) + k_P P_Z - k_L L_Z \quad (1)$$

$$dP_Z/dt = -\rho_P(P_Z - P_\infty) + k_L L_Z - k_P P_Z \quad (2)$$

where L_Z and P_Z denote the lactate and pyruvate signals; t is time; P_∞ and L_∞ correspond to the equilibrium signal at time ∞; k_P and k_L are the apparent rate constants that include T_1 decay, delivery, and membrane transport kinetics. The relaxation rates (ρ_P, ρ_L) in this model are assumed to be the same for pyruvate and lactate.

Both dynamic spectroscopy experiments were fit after a delay to properly account for the CA injection timing relative to the [1-^{13}C] pyruvate injection. The resultant values from the model fitting were then compared to demonstrate potential differences in estimated rates of lactate production. For the brain experiments, the concentration of CA in the brain following a bolus injection was assumed based on literature [18] for simulation, but the simultaneous acquisition described below enabled real-time measurement of local T_1 times to further improve the modeling precision.

G. Simultaneous Imaging of ^{1}H and ^{13}C

In order to directly measure the regional concentration of the CA, a simultaneous ^{1}H and ^{13}C acquisition was developed in order to provide an independent measure of the CA effect on T_1-shortening of protons within the biological compartments. A technique to monitor the concentration of the CA *in-vivo* using a bookend T_1 signal intensity modulation technique [12] was combined with simultaneous measurement of hyperpolarized ^{13}C tracer metabolism in a third rat. This dynamic multi-nuclear MRSI technique provides several advantages by providing complementary information in order to constrain the signal modeling.

This technique allowed a more realistic model by providing contrast to the compartments that represented the vascular and extracellular/extravascular spaces using (3):

$$\frac{1}{T_{1,eff}} = \frac{1}{T_1} + r_1 \times [CA] \quad (3)$$

where [CA] is the concentration (mM) of the gadolinium contrast agent. The relaxivity (r_1) of the specific CA used for [1-^{13}C] pyruvate was measured in separate experiments at 4.7T and found to be 0.19 ± .01 $s^{-1}mmol^{-1}$.

III. Results

A. ^{13}C Acquisitions

The dynamic spectra that were acquired in the first two experiments are shown in Fig. 1a. The increased relaxation of the spectra after gadolinium injection is apparent compared to the spectra without the sequential CA injection. Fig. 1b compares the normalized pyruvate and lactate dynamics for both experiments. Following the CA injection (t = 18 s), the pyruvate signal decay rate significantly increases and the lactate signal shows a similar response. After a short time for both mixing of the circulation and spin-lattice exchange between the CA and vascular ^{13}C spins, qualitatively the signal decay stabilizes to a new exponential decay rate. Compartmental modeling of the two experiments (Fig. 2) revealed a

significant difference in the apparent metabolic rate constants. In Table I it is noted that the apparent metabolic rate constant k_P increased markedly after eliminating signal from the vascular compartment. The kinetic measures of metabolism in the liver require a more complex model due to the inclusion of an extravascular compartment in the absence of a blood-brain barrier.

B. Simultaneous ^{13}C and ^{1}H Imaging

As is seen in Fig. 3, the simultaneous acquisition of both the hyperpolarized [1-^{13}C] pyruvate as well as the ^{1}H signal allows for the localization of the dynamic information for both channels. This is shown in Fig. 3a where both the [1-^{13}C] pyruvate intensity and concentration of CA are plotted together to show the extracellular depolarization of the hyperpolarized ^{13}C signal caused by the CA in those regions. The images in Fig. 3a–b show two stages in the dynamic time course of the experiment with the [1-^{13}C] pyruvate data overlaid on the ^{1}H data. Fig. 3a shows a time point before the CA has reached the liver. Fig. 3b shows a time point after the CA has depolarized most of the ^{13}C signal in the vascular space, while the signal in the tissue remains high.

C. Modeling of gadolinium based on prior calculation

A more realistic model that distinguishes a vascular compartment is presented in Fig. 4a. An input function based on literature [18] and applied to the data from the brain using this model results in good agreement between the model and data (Fig. 4b) and is hypothesized to reflect a more precise representation of the metabolite dynamics.

IV. Discussion

In-vivo metabolic studies using HP ^{13}C compounds raise significant challenges for quantitative measurement of cellular metabolism due to inadequate compartmental characterization using conventional simplified kinetic modeling methods. Therefore alternative strategies that resolve signal from different compartments and provide additional constraints through independent measures of vascular perfusion are needed to accurately estimate both membrane transport and intracellular chemical exchange. This work demonstrates that injection of a T_1-shortening agent following a ^{13}C-pyruvate injection not only provides contrast to isolate the intracellular ^{13}C signal *in-vivo*, but can provide perfusion and local T_1 relaxivity information when the dynamic ^{1}H and ^{13}C signals are acquired simultaneously [17]. A potential disadvantage of Gd-chelates is that they accelerate decay of the polarized substrate (e.g. pyruvate). This trades off signal to noise in exchange for quantitative accuracy. This tradeoff may not always be desirable, especially if quantitative precision is not required for a given application.

Future work will investigate sensitivity to model parameters and different concentrations and relaxivities of CA and to extend the modeling to body organs such as the liver where the extravascular compartment must be considered. Another important avenue for future research is to include other T_1-shortening contrast agents with different but known volumes of distribution for applications in healthy and diseased models.

Acknowledgments

This work was supported in part by the NIH/NCI under Grant 5 T32 CA009206-28 and NIH/NIA P50AG033514 as well as GE Healthcare.

We thank GE Healthcare for support and Beth Rauch for help with animal preparation.

References

1. Chen AP, et al. Hyperpolarized C-13 spectroscopic imaging of the TRAMP mouse at 3T-initial experience. Magn Reson Med. 2007; 58(6):1099–106. [PubMed: 17969006]
2. Hu S, et al. In Vivo Carbon-13 Dynamic MRS and MRSI of Normal and Fasted Rat Liver with Hyperpolarized (13)C-Pyruvate. Mol Imaging Biol. 2009; 11(6):399–407. [PubMed: 19424761]
3. Hu S, et al. Compressed sensing for resolution enhancement of hyperpolarized 13C flyback 3D-MRSI. J Magn Reson. 2008; 192(2):258–64. [PubMed: 18367420]
4. Day SE, et al. Detecting tumor response to treatment using hyperpolarized 13C magnetic resonance imaging and spectroscopy. Nat Med. 2007; 13(11):1382–7. [PubMed: 17965722]
5. Zierhut ML, et al. Kinetic modeling of hyperpolarized 13C1-pyruvate metabolism in normal rats and TRAMP mice. Journal of Magnetic Resonance. 2010; 202(1):85–92. [PubMed: 19884027]
6. Harris T, et al. Kinetics of hyperpolarized 13C1-pyruvate transport and metabolism in living human breast cancer cells. Proceedings of the National Academy of Sciences. 2009; 106(43):18131–18136.
7. Weidensteiner C, et al. Imaging of intracellular sodium with shift reagent aided 23Na CSI in isolated rat hearts. Magnetic Resonance in Medicine. 2002; 48(1):89–96. [PubMed: 12111935]
8. Larson P, et al. Hyperpolarized 13C 3D Metabolic Imaging with Stimulated Echoes for Flow Suppression. Proc ISMRM. 2010:2410.
9. Ardenkjær-Larsen JH, et al. Increase in signal-to-noise ratio of > 10,000 times in liquid-state NMR. Proceedings of the National Academy of Sciences of the United States of America. 2003; 100(18): 10158–10163. [PubMed: 12930897]
10. Comment A, et al. Design and performance of a DNP prepolarizer coupled to a rodent MRI scanner. Concepts in Magnetic Resonance Part B: Magnetic Resonance Engineering. 2007; 31B(4):255–269.
11. Golman K, et al. 13C-angiography. Acad Radiol. 2002; 9(Suppl 2):S507–10. [PubMed: 12188323]
12. Cron GO, Santyr G, Kelcz F. Accurate and rapid quantitative dynamic contrast-enhanced breast MR imaging using spoiled gradient-recalled echoes and bookend T1 measurements. Magnetic Resonance in Medicine. 1999; 42(4):746–753. [PubMed: 10502764]
13. Gabellieri C, Leach MO, Eykyn TR. Modulating the relaxivity of hyperpolarized substrates with gadolinium contrast agents. Contrast Media & Molecular Imaging. 2009; 4(3):143–147. [PubMed: 19330792]
14. Bell LC, et al. Dual-Tuned 1H/13C Orthogonal Double Solenoid Volume Coil for Simultaneous Acquisition in Small Animals In Vivo. Proc ISMRM. 2010:7112.
15. Harris FJ. On the use of windows for harmonic analysis with the discrete Fourier transform. Proceedings of the IEEE. 1978; 66(1):51–83.
16. Chen L, et al. An efficient algorithm for automatic phase correction of NMR spectra based on entropy minimization. Journal of Magnetic Resonance. 2002; 158(1–2):164–168.
17. Peterson ET, et al. Simultaneous Proton and Hyperpolarized Carbon Imaging. Proc ISMRM. 2011:449.
18. Yang C, et al. Estimating the arterial input function using two reference tissues in dynamic contrast-enhanced MRI studies: Fundamental concepts and simulations. Magnetic Resonance in Medicine. 2004; 52(5):1110–1117. [PubMed: 15508148]

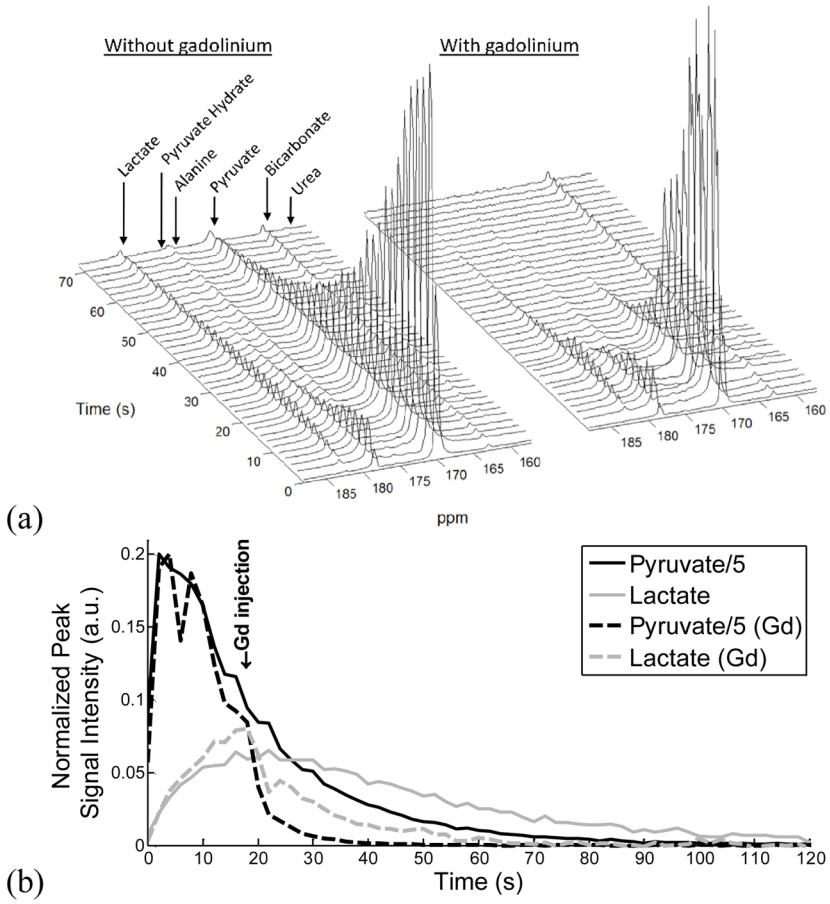

Fig. 1.

(a) Dynamic spectra (every third spectrum shown) acquired from rat brain following injection of [1-^{13}C] pyruvate without and with the injection of gadolinium. The dynamics reveal the T_1-shortening effect (increased relaxivity) of the gadolinium. (b) The dynamic peak intensities of the pyruvate and lactate peaks normalized to pyruvate. The experiment with the gadolinium injection (dotted lines) shows increased relaxivity but not complete elimination of the pyruvate and lactate signals, implying elimination of the signals at a compartment specific level. In the case of healthy brain, the signal within the vascular compartment is eliminated.

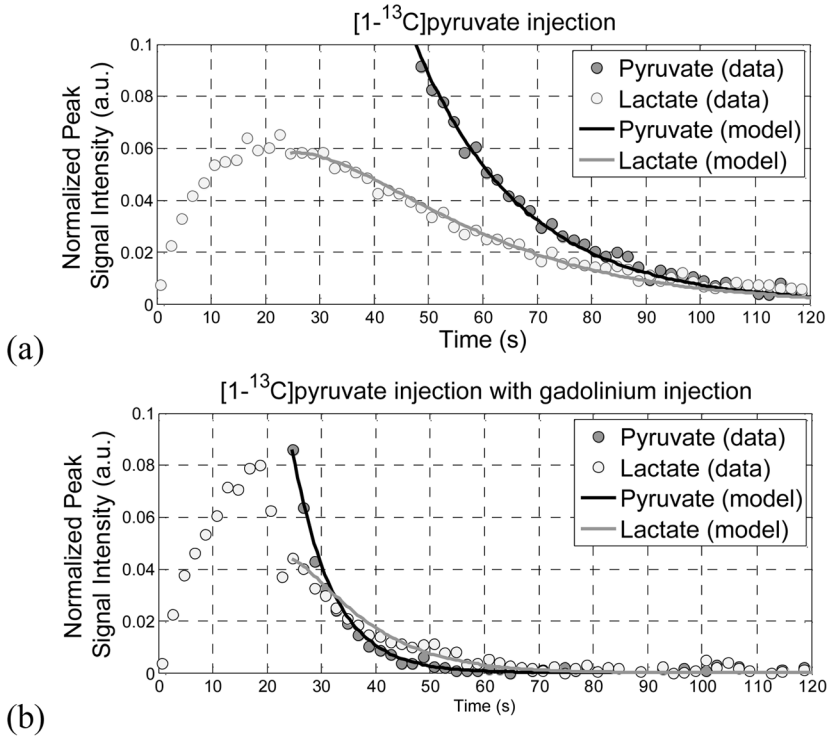

Fig. 2.

The two-compartment model describing the evolution of the hyperpolarized ^{13}C label after injection was fit to the experiment with (a) and without (b) the gadolinium injection.

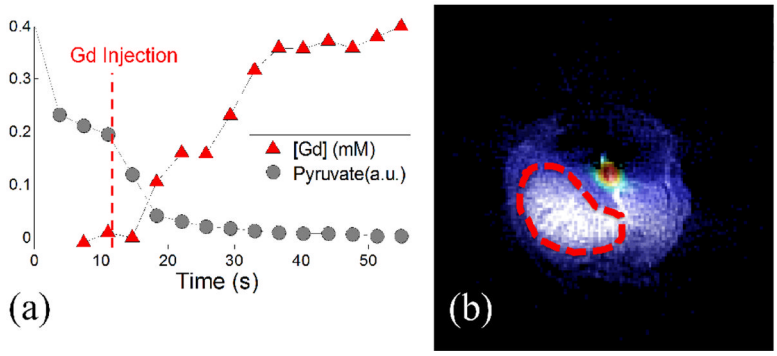

Fig. 3.

In-vivo T_1 monitoring using a gadolinium-based contrast agent. (a) Gd concentration and pyruvate signal intensity over time in the liver of a rat (indicated in b). (b) An image of ^{13}C-pyruvate shown overlaid on the ^{1}H image for the same experiment prior to the contrast agent injection (t = 8 s).

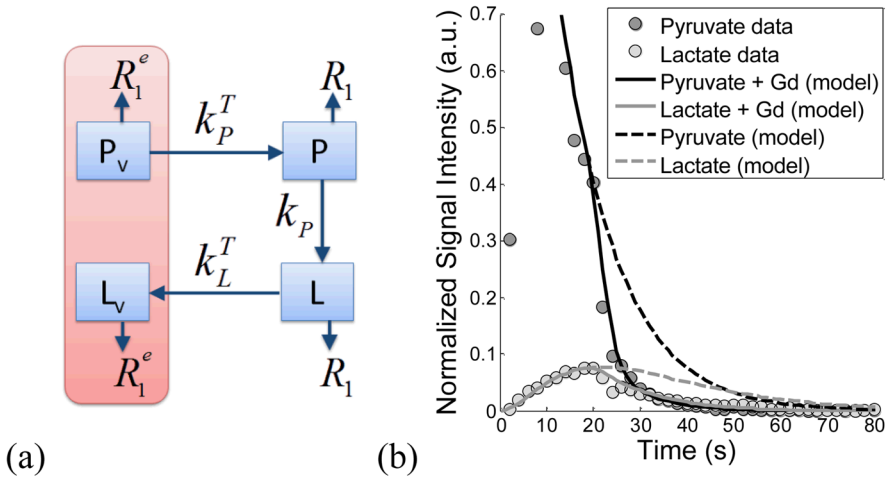

Fig. 4.

(a) A four compartment model, which is an extension of the two compartment model [4], allows for the modeling of the increased relaxation due to a sequential CA injection within the vascular compartment. (b) A simulation of the compartment specific T_1-shortening effect using a simulated CA input function compares well with the measured data. The inclusion of the CA into the model allows a more complete use of the data acquired.

TABLE I

Compartmental Modeling of ^{13}C Metabolic Dynamics

Experiment	k_P
Animal 1	
Pyruvate only	0.008
Pyruvate + gadolinium	0.022
Animal 2	
Pyruvate only	0.008
Pyruvate + gadolinium	0.034